Proton-Proton Scattering at 31.8 Mev, Proportional Counter Method*

BRUCE CORK, LAWRENCE JOHNSTON,** AND CHAIM RICHMAN
Radiation Laboratory, University of California, Berkeley, California
(Received February 20, 1950)

Differential cross-section measurements for proton-proton scattering have been made with protons of 31.8-Mev incident energy, scattered from hydrogen at one atmosphere pressure. Seven increments of angles from 15° to 51° in the laboratory system of coordinates have been measured simultaneously using proportional counters. In order that measurements could be made with very small currents, axially symmetrical defining slits and counters were made to include large solid angles. A 90° coincidence method was also used at large angles to give an independent geometry and to detect the possibility of slit and contamination scattering. The ratio of the differential cross section at 30° to that at 90°, center of mass system, is observed to be compatible with pure S-wave scattering of approximately 50° phase shift.

INTRODUCTION

THE scattering of protons on protons has been carried out by many investigators at successively higher energies,[1–13] and the analysis[14–19] of these experiments has provided us with a phenomenological picture of the nuclear interaction between two protons. The experiments which have been carried out so far which use protons of incident energy up to 14.5 Mev can all be explained on the basis of pure S-wave scattering. If there are effects in this energy region due to the scattering of the P-wave they appear to be small. It was very desirable therefore that experiments be made at higher energies to see if one could observe the scattering of the higher angular momentum waves. With the completion of the Berkeley linear accelerator such an experiment became possible.

The Berkeley linear accelerator[20] gives an external beam of well-collimated 32-Mev protons. This makes it practically an ideal machine with which to do scattering experiments. Two independent experiments were undertaken. One experiment, performed by Panofsky and Fillmore, uses nuclear emulsions as detectors of the scattered protons. The second experiment which is described below uses proportional counters to detect the scattered protons, and a completely different geometry. The apparatus was designed and constructed before the linear accelerator was completed. Since the magnitude of the anticipated beam was not known it was desirable to construct the apparatus so that as many of the scattered protons would be detected as possible.

Each proportional counter was thus constructed to intercept as large a solid angle as conveniently possible, and the scattering into seven angular intervals was measured simultaneously. To determine the internal consistency of the data, two different scattering geometries were used simultaneously, namely "singles" and "90° coincidence." By singles is meant that a count is registered every time a single proton goes into a particular counter. The scattering geometry for the singles is defined by the two coaxial cylinders and the zonal apertures of the individual counters as shown in Fig. 2.

When identical particles collide elastically their trajectories are at 90° to each other (including relativistic effects for 32-Mev incident protons the angle is 89.6°) in the laboratory system. Thus, a proton-proton collision can also be measured as a 90° coincidence by arranging the counters in the proper manner. The 90° coincidence[7] method is included for large angles to investigate the possibility of errors caused by slit scattering and contamination scattering, to reduce the effective background counts, and to give a geometry independent of the geometry of the singles counting method. The coincidence method depends only on the entrance apertures to the coincidence counters for the definition of the geometry.

DESIGN OF SCATTERING APPARATUS

The complete scattering apparatus is shown in Fig. 1. With one atmosphere of hydrogen in the scattering chamber a current of 10^{-13} ampere is sufficient to give a good counting rate of scattered protons. The accelerator was found capable of accelerating more than 10^5 times this amount of current. The protons were made

* This work was performed under the auspices of the AEC.
** Now at the University of Minnesota, Minneapolis, Minnesota.

[1] H. W. Wells, Phys. Rev. **47**, 591 (1935).
[2] M. G. White, Phys. Rev. **49**, 309 (1936).
[3] Tuve, Heydenburg, and Hafstad, Phys. Rev. **50**, 806 (1936).
[4] Hafstad, Heydenburg, and Tuve, Phys. Rev. **53**, 239 (1938).
[5] Heydenburg, Hafstad, and Tuve, Phys. Rev. **56**, 1078 (1939).
[6] Herb, Kerst, Parkinson, and Plain, Phys. Rev. **55**, 998 (1939).
[7] R. R. Wilson, Phys. Rev. **71**, 384 (1947).
[8] R. R. Wilson and E. C. Creutz, Phys. Rev. **71**, 339 (1947).
[9] Wilson, Lofgren, Richardson, Wright, and Shankland, Phys. Rev. **71**, 560 (1947).
[10] Dearnly, Oxley, and Perry, Phys. Rev. **73**, 1290 (1948). J. Rouvina (private communication).
[11] Blair, Freier, Lampi, Sleator and Williams, Phys. Rev. **74**, 553 (1948).
[12] Ragan, Kanne, and Taschek, Phys. Rev. **60**, 628 (1941).
[13] Bondelid, Bohlman, and Mather, Phys. Rev. **76**, 865 (1949).
[14] Yost, Wheeler, and Breit, Phys. Rev. **49**, 174 (1936).
[15] Breit, Condon, and Present, Phys. Rev. **50**, 825 (1936).
[16] Breit, Thaxton, and Eisenbud, Phys. Rev. **55**, 1018 (1939).
[17] Hoisington, Share, and Breit, Phys. Rev. **56**, 884 (1939).
[18] H. A. Thaxton and L. Hoisington, Phys. Rev. **56**, 1194 (1939)
[19] H. A. Bethe, Phys. Rev. **76**, 38 (1949).
[20] Bradner, Crawford, Gordon, and Woodyard, Phys. Rev. **73**, 534A (1948).

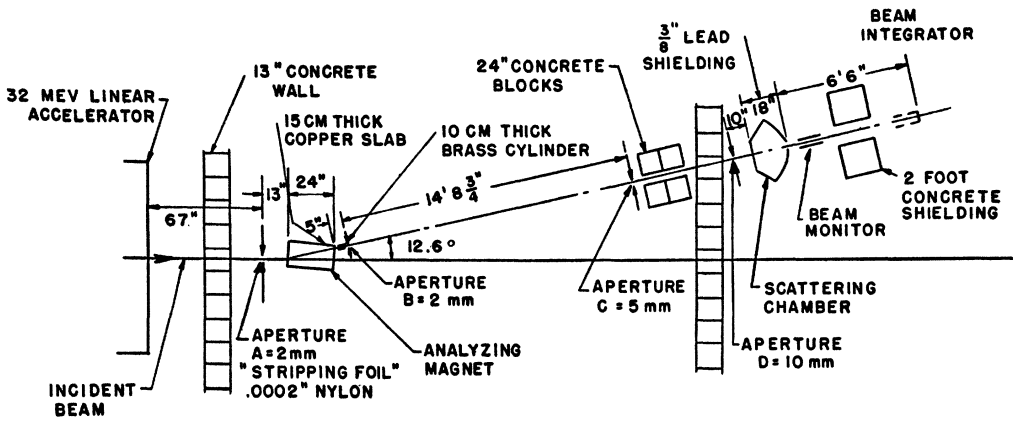

FIG. 1. General arrangement of apparatus.

monoenergetic by means of an analyzing magnet, and advantage was taken of the large available current to further collimate the beam to ± 0.05 degree by means of a slit system and tube approximately 5 meters long.

The scattering chamber is shown in Fig. 2. The proton beam is incident from the left and scattered from the region defined by two coaxial cylinders. In order that a favorable solid angle for detection of the scattered protons will result, the proportional counters have been made to detect simultaneously all protons scattered into various zones of a sphere. The two angle-defining cylinders limit the source of the scattered protons, and these plus the zonal apertures define the singles scattering geometry.

Since it is desirable to evacuate the scattering chamber and the proportional counter independently, considerable care was necessary in the mechanical design of the supporting structure. The main body of the chamber is constructed of a welded cone of cold-rolled steel $\frac{3}{8}$ in. thick and nickel plated. Supporting struts (see Fig. 2) were likewise made of welded cold-rolled steel in the form of cones coaxial with the main body cone. These were spaced at the dividing zones of the increments of angle by radial struts which are welded to the main center hub.

The angle-defining plate, which is a section of a sphere, was carefully machined on a lathe, starting with a 600-pound slab of cold-rolled steel. The critical dimensions of the apparatus are thus determined by the dimensions of this plate and can be easily measured.

All of the windows for the counters were made by inserting a single 0.025 in. aluminum spinning over the angle-defining plate. Ring-type rubber gaskets sealed the scattering chamber and the counter chamber to the aluminum spinning. The counter chamber was made of a heavy aluminum spinning with conical aluminum partitions between the counters. Aluminum absorbers (see Table II) were placed in the small-angle counters to degrade the energy of the protons and increase their specific ionization. These absorbers also kept slit-scattered protons of low energy from penetrating into the counters.

Each counter is a torus of approximately a rectangular cross section, and the collecting electrode consists of a 0.002-in. diameter tungsten wire supported by 12 radial silk threads.

The 45° counter is split azimuthally into two 180° sectors, top and bottom, so that 90° coincidence between the top and bottom halves results. Likewise, the 39° and 51° counters are arranged so that the top-half of the 51° counter will give a 90° coincidence with the bottom half of the 39° counter, and vice versa.

Two 0.0002 in. Nylon foils rotated so that the "grain" in each is lined up at 90° to the other, form the diaphragm separating the hydrogen system from the linear accelerator. Hydrogen is admitted through a palladium leak to the collimator (Fig. 2) and allowed to diffuse through the scattering region. Most of the incident protons continue on through the chamber and are collected in the charge integrator, which will be described later. For convenience in sending beam-monitoring information back to the accelerator control desk, an ionization chamber has been included as indicated.

A mechanical shutter shown in Fig. 2, consisting of a cylinder, coaxial with the defining cylinders, is operated through a Wilson seal. Background runs are made with this shutter moved to the forward position, so that the aperture between the defining cylinders is closed.

DETECTION OF SCATTERED PROTONS

The signals from the proportional counters were transmitted through Kovar seals with Kovar guard rings to the grid of a 4-tube amplifier and cathode follower. The gas multiplication was approximately 100, but was changed during the process of determining the plateau for detecting all the scattered protons, which will be discussed in more detail later. The maximum gain of the 4-tube amplifier was 3000; the band-width was 0.9 megacycle. The output from each cathode follower operated a 5-tube channel consisting of a variable discriminator, gate tube, and scale of 4, with mechanical register. Signals from the 51°, 45°, and 39° discriminators were also sent to 3 coincidence units and to one unit that measured the number of accidental coincidences.

The resolving time of the singles scaling circuit is limited by the discriminator circuit. This resolving time was measured using a double-pulse signal generator, and it was observed that two signals closer than 5 microseconds will be counted as a single count. The resultant correction to our data was always less than 2 percent.

The mechanical registers used with the scale of 4 units are known to be reliable for 15 impulses per second, but of course they will not register two impulses during the same 300 microsecond interval. The counting rate was sufficiently small that, on the average, the mechanical register operated only once in eight pulses of the linear accelerator, making negligibly small the chance of getting two (scaled×4) impulses during a linear accelerator pulse.

MEASUREMENT OF ENERGY

The diameters of the collimators (Fig. 1) are as follows: A, 2.0 mm; B, 2.0 mm; C, 5.0 mm; D, 10 mm; E, 12 mm. Collimators A, B, and C used in conjunction with the magnet allow the proton energy to be selected to ± 0.5 Mev. The integral of the magnetic field along the trajectory of the protons has been measured to $\pm\frac{1}{2}$ percent by a group working with Mr. Duane Sewell. This plus the angular deflection of the beam is sufficient[21] to define the energy of the beam. The energy was also measured using proportional counters coincident in depth, plus aluminum absorbers to obtain first an integral curve and then a differential absorption curve. Each of these methods gives an energy of 31.8 ± 0.3 Mev for the incident beam, corrected for energy loss in the nylon foil and hydrogen.

Since some ionized hydrogen molecules are accelerated to 16 Mev by the accelerator, it is necessary to insert a thin foil ahead of the magnet to "strip" the molecule, thus changing its charge to mass ratio so that it will not have the same $H\rho$ as a 32-Mev proton. A 0.0002 in. nylon foil mounted at collimator A was used to accomplish this stripping.

MEASUREMENT OF INCIDENT PROTON FLUX

The beam-integrating equipment is shown physically in Fig. 3 and electrically in Fig. 4. Protons enter the

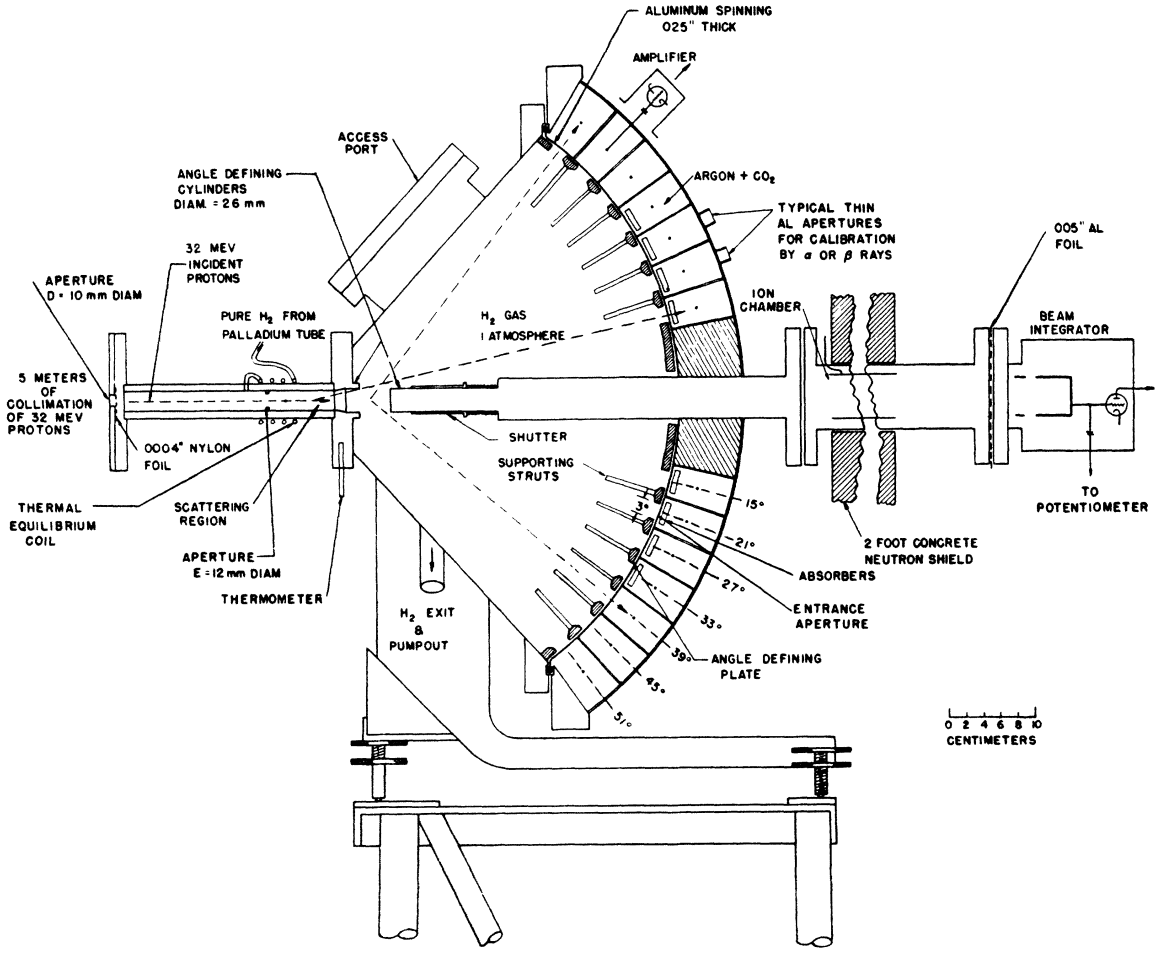

FIG. 2. Proton-proton scattering chamber.

[21] R. R. Wilson and E. C. Creutz, Rev. Sci. Inst. **17**, 385 (1946)

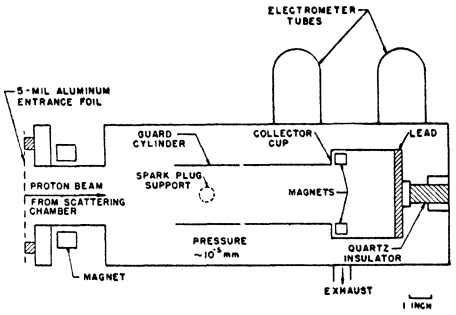

FIG. 3. Mechanical layout of charge integrator.

high vacuum region of the collector through a 5-mil aluminum foil and pass through a guard cylinder into the collector cup, where they are stopped in lead. The guard cylinder is maintained at -200 volts in order to trap secondary electrons, which are produced by the beam at the aluminum entrance foil and in the cup. As an added precaution against secondaries, small permanent magnets were mounted at the foil and in the cup to produce a field of about 50 gauss at the proton path.

The size of the beam and its orientation in the cup were determined by exposing an x-ray film to the beam, indicating that the beam was quite well defined with a diameter of about 2 centimeters. Clearances were considered adequate to the walls of both the cup and the guard cylinder.

The integrator circuit (Fig. 4) functions as follows: Protons collected in the cup charge the condenser $C_1=0.001071$ microfarad, causing a voltage V to appear across it. The charge is calculated as V times C_1. V is measured by manually adjusting the standard potentiometer P_1 to make the cup remain at ground potential, whereupon V is read as the voltage on the potentiometer dial. The electrometer tube and galvanometer comprise a vacuum tube voltmeter which is used as a null instrument to indicate when the cup is at ground potential. It will be seen that the potentiometer needs to be adjusted accurately only at the beginning and end of a run; it was kept in rough adjustment during a run, however, to monitor the collected charge.

To avoid errors due to stray lead capacitance and possible sensitivity to air pressure it was decided to measure the integrating capacitor C_1 in its operating position in the vacuum chamber. The effective capacitance for beam integration is the mutual capacitance between the cup and the potentiometer lead marked A, and is independent of the capacitance of either to ground; this was measured by comparison with a standard variable air condenser both at 1000 cycles and at very low frequency (actually d.c. impulses about 5 seconds long) by suitable bridges. These checked to within 0.2 percent, which was taken as the limit of short-time soakage in the condenser. Long-time soakage and leakage were also shown to be less than 0.1 percent for half-hour runs. The calibration of the variable condenser was also checked against a standard mica condenser at 1000 cycles. C_1 is a polystyrene insulated unit, made by the Fast Company. A series of $p-p$ scattering runs was made as a function of the potential on the guard cylinder, and another set as a function of gas pressure in the integrator, from which it was concluded that errors due to secondary electrons and gas multiplication would be negligible. The grid current of the electrometer tube was measured after each series of runs for which a correction of approximately one percent was necessary. We have assigned a probable error of $\pm\frac{1}{2}$ percent to the beam measurements. This integrator was developed by Mr. Lee Aamodt, to whom we are indebted.

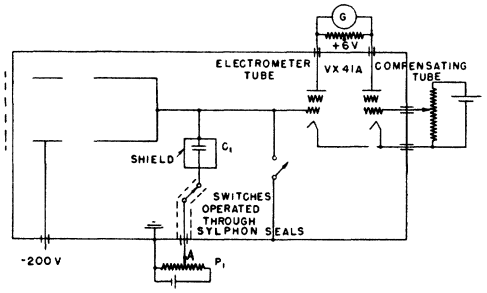

FIG. 4. Electrical circuit of charge integrator, slide-back type of potentiometer.

HYDROGEN GAS SUPPLY

Pure hydrogen gas for the scattering chamber was obtained by passing tank hydrogen through a heated palladium thimble. This device is similar to the one described in the preceding paper and hence will not be discussed. Before entering the chamber, the gas passes through a coil of copper tubing wrapped around the collimator tube, to insure thermal equilibrium with the walls of the chamber. The temperature is measured by a thermometer embedded in the flange of the collimating tube during a run. All joints in the tube carrying gas from the palladium tube to the chamber are made without rubber gaskets, using either metal flared fittings or threaded joints waxed with Cenco "Sealstix." Hydrogen enters the chamber in the middle of the collimator and from there flows continually out into the main volume of the chamber. It will be seen that most of the scattering takes place in the interior of the collimating tube where the hydrogen is most pure; this is particularly true of scattering at small angles, where the effects of Coulomb scattering from contaminating gases are most likely to be encountered. The excess hydrogen escapes from the chamber via an oil-lock tube which regulates the pressure and prevents back-

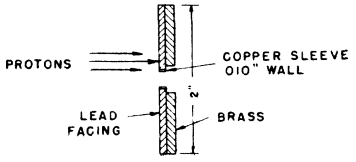

FIG. 5. Circular apertures, arranged with lead facing to reduce the neutron background.

TABLE I. Scattering data. Geometrical scattering length = 5.38 cm. Normalized for collected charge = 317.1×10^{-12} coulombs. Mean energy = 31.8±0.3 Mev. 89.7° T and B refers to top half and bottom halves of a given counter. All counts ×4.

Run	Date	Counter potential volts	Singles mean angles, center of mass 89.7°T	89.7°B	77.6°B	64.7°	52.5°	39.8°	27.3°	Av. back-grnd. %	$Q \times 10^{-12}$ coulombs	Coincidence angles (center of mass) 90°−90°	102°−78°
1	7-15-49	3200*	590	623	582	1072	—	728	492	21	316	136	—
2		3200*	623	585	594	1061	929	706	494	28	316	132	138
3		3100*	625	625	600	1077	—	720	480	11	316	140	134
4		3100*	590	612	617	1085	—	690	494	13	316	138	139
5		3000	585	597	561	1125	—	641	459	10	316	127	128
6		3000	623	599	596	1088	—	668	447	5	316	134	137
7		3000	618	612	610	1084	—	677	474	5	316	138	136
8		2800	612	604	516	1016	—	616	416	2	316	128	124
9		Av. values	607	611	598	1074	(929)	711	490		1.264	136.5	137
10	7-22-49	3100*	655	630	602	1068	977	705	497	54	318	157	141
11		3000*	613	623	585	1039	948	713	485	25	318	140	141
12		3000*	614	647	601	1110	971	715	506	34	318	136	135
13		Av. values	628	633	596	1072	965	711	496		954	144	139
14	8-29-49	2700*	574	594	584		925	707	470	24	317	139	141
15		2700*	627	631	586		940	729	502	19	317	153	138
16		2700*	599	622	599		938	743	515	33	317	153	142
17		Av. values	600	616	590		934	726	496		951	148	140
18	9-1-49	2900*	607	607	598	1055	—	674	486	25	211	141	139
19		2800*	611	623	610	1091	—	742	514	25	211	153	142
20		2800*	657	625	608	1145	—	706	506	20	211	144	138
21		2800*	596	595	603	1059	—	710	485	26	211	126	135
22		2800*	582	606	589	1106	—	727	470	21	211	131	147
23		Av.	611	611	602	1091	—	712	492		1055	139	140
24	9-8-49	2800*	603	626	603	1151	963	745	512	35	211	139	139
25		2800*	595	605	606	1114	947	690	512	35	211	129	138
26		Av.	599	615	605	1132	955	717	512		422	134	139
27		Wtd. mean	610.1	616.9	597.5	1085	943	715	494.9			140.7	138.9
28		RMS Dev.	±.77	±.59	±.38	±1.1	±.78	±.36	±.70			±1.6	±.35
29		G factor	0.3108		0.3128	0.3444	0.3955	0.4937	0.7054			2.685	2.710
30		Abs. $(d\sigma/d\Omega)$c.m.	14.30		14.05	14.05	14.02	13.27	13.13			14.21	14.15
31		Prob. error (differential)	±1.1%		±1.1%	±1.4%	±1.2%	±1.1	±1.2			±1.8%	±1.1%

diffusion of air into the system. The hydrogen flow normally used was sufficient to change the gas completely in 90 minutes; this swept out contaminating gases evolved from the chamber walls with sufficient speed. Tests for determining gas contamination will be described in a later section.

BACKGROUND EVALUATION

Reduction of background counts was the greatest single difficulty encountered in doing this experiment, and it is felt that anyone starting to work with protons of this energy or above would do well to use coincidence counter telescopes, and fast circuits. By carefully shielding against x-rays and neutrons we were able to obtain data with a background of about 20 percent. Of this background, about $\frac{1}{4}$ is x-rays and $\frac{3}{4}$ neutrons.

The x-rays are generated by stray electrons accelerated to a few hundred kilovolts between the drift tubes of the linear accelerator. These were effectively reduced by covering the scattering chamber with $\frac{3}{8}$ in. of lead. The neutrons are produced wherever the beam strikes matter, with only slight dependence on the nuclear species. Rough experiments indicated that lead and bismuth gave approximately $\frac{1}{2}$ the background effect observed in carbon, copper or aluminum. Hence lead was used to stop the protons wherever practicable. A typical collimator disc is shown in Fig. 5. Most of the protons to be rejected by the disk strike the lead facing, while the hole itself is lined with a thin collar of copper to reduce scattering from the collimator edge.

The neutron flux at the counters is greatly reduced also by arranging the collimating system so that all protons to be rejected are stopped at some distance from the counters, and several feet of concrete are interposed between the counters and the last collimating disc. Note that the main proton beam does not strike any solids after collimator C, until it is stopped in lead at the integrator. The integrator is placed 6 feet behind the counters, in order to allow extra concrete shielding between them.

Background caused by cosmic rays and other accelerators in the vicinity was reduced to a very small

TABLE II. Absorbers installed in counter windows.

(Laboratory system) θ_{max}	θ_{min}	Total aluminum absorber mg/cm²	Residual range of 31-Mev incident proton mg/cm² Al
16.31°	11.00°	867	183
23.05°	16.76°	709	116
29.71°	22.51°	530	230
36.36°	28.49°	351	229
43.24°	34.39°	179	221
49.67°	40.00°	179	81
56.38°	46.00°	179	—

fraction of the total background by gating on the counters only during a pulse of the linear accelerator.

Since the background was large, it had to be evaluated accurately; and unfortunately the background varied with time by as much as 25 percent. Thus a single background run would not give a good correction. It was necessary to break up the running time into a series of short scattering runs alternated with background runs, so that the fluctuations in background would average out over the series. The only assumption necessary here is that background fluctuations are random with regard to whether the run is for measuring scattering or background, and we feel that this condition has been fulfilled. Background variations were caused by the operating conditions of the accelerator, and hence one might suspect that the accelerator crew would have been more careful in their operation during a scattering run than during a background run. Accordingly, precautions were taken to insure that the crew would not find out during a series, which runs were for background. The general background level in the room was continuously monitored by an auxiliary proportional counter of geometry similar to the proton counters and located adjacent to the scattering chamber. The readings on this counter were used to approximately normalize each background run to the general background level during the preceding scattering run. By these devices we were able to reduce to about $\frac{1}{2}$ percent the effect of background variation on our results, as judged from the internal consistency of the series of five runs listed in Table I.

A further item of importance is to show that the true background is being measured, i.e., that closing the shutter to cut off the scattered protons from the counters does not appreciably change the background counts.

The two principal avenues by which this could occur are here discussed: 1. Hydrogen-scattered protons which normally are counted, or which strike opaque zones of the steel defining plate, will instead strike the shutter and make a nuclear reaction which can produce a count. This will be a small effect, since such a nuclear reaction will have a yield of about 10^{-5}, and the resulting particles will be counted with low efficiency by the counters. 2. Any neutrons which enter the chamber co-linearly with the incident proton beam could produce $n-p$ scattering in the H_2 gas, which would be recorded as $p-p$ scattering since the shutter would cut out the scattered protons during background runs. In all counters, except the 77.6° one (all angles are expressed in the center of mass system), protons would not have sufficient energy to penetrate the absorbers placed in the counter windows unless they were scattered from neutrons of at least 22 Mev energy. The corresponding minimum neutron energy at the 77.6° counter is 18 Mev. We have shown in another experiment that the yield of high energy neutrons by 32-Mev proton bombardment on copper or lead is less than 10^{-6} using the carbon $(n, 2n)$ reaction as the detector. This reaction has a neutron threshold of 20 Mev. The most likely place for these neutrons to be produced is at collimator C, and, allowing that 100 times as much beam is stopped at this collimator as is transmitted, and that the neutrons generated spread out with a full angle at $\frac{1}{2}$ intensity of 10°, the neutron intensity inside the defining cylinders is less than 10^{-6} of the incident proton beam. Since $n-p$ and $p-p$ scattering cross sections are comparable in magnitude, $n-p$ scattered protons will be less than 10^{-6} of the $p-p$ scattered ones. The above is consequently a negligible source of error.

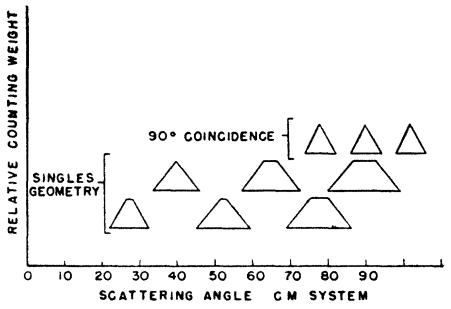

FIG. 6. Weighing factors of various counters.

EVALUATION OF PROTONS SCATTERED FROM SLITS, GAS CONTAMINATION, ETC.

Reference to Fig. 2 will show that it is impossible for a primary proton to scatter from the Nylon foil or any of the metal apertures and get into a counter, without scattering once more in the process from another body. The probability of such an event is rather complicated to calculate, so we relied on experiments in which we looked for residual scattering counts when the chamber was highly evacuated. No effect was observable above background. Thus this source of error would be less than 1 percent at all angles.

A possible event not covered by the above experiment would be that protons, scattered from hydrogen gas near the entrance foil at small angles, would strike the defining cylinders and thence bounce into a counter.

To test this, it was necessary to have hydrogen atoms in the collimating tube to illuminate the edges of the defining cylinders with scattered protons, but it was also necessary to have no hydrogen in the scattering region from which "honest" scattered protons could reach the counters. This was arranged by placing an extra nylon foil 5 mils thick in the collimating tube at the plane of collimator E (Fig. 2). This foil is calculated to produce Rutherford scattering equivalent to filling the collimating tube with 100 atmospheres of H_2 gas. Residual scattering was now looked for with the chamber evacuated, but none was observed. One atmosphere of H_2 gas normally present in the collimator will produce less than a 0.1 percent error in the 27.3° counter, due to this event.

To determine the tolerance on gas impurities for this

experiment, the scattering of 32 Mev protons in air was measured with the same apparatus. From this we concluded that our hydrogen should contain less than 0.01 percent of nitrogen or oxygen in order to reduce the resultant scattering to 0.1 percent of the $p-p$ scattering. To determine the rate of evolution of contaminating gases from the chamber walls, the chamber was evacuated before each run, and the rate of increase of pressure measured on the chamber with the (cold) palladium tube connected. This rate never exceeded 10^{-5} atmospheres per hour, which, combined with the hydrogen flushing period of $1\frac{1}{2}$ hours, gives a maximum impurity content of 0.001 percent for the gas in the main chamber. Thus the feature of introducing the pure hydrogen gas into the scattering region of the chamber is not absolutely necessary, but it does provide a gross experimental check on the contamination of the main chamber, as follows:

At the end of a series of runs, a run was made in which the supply of pure hydrogen was cut off, so that any contamination in the main chamber would diffuse into the scattering region. The measured cross section was the same, to within its probable error of 2 percent, as in the runs in which the gas was flowing. The palladium tube was tested for perforation before and after each series of runs. In view of the measured low rate of evolution of contaminating gases, and the continuous renewal of hydrogen in the scattering region, we consider the scattering due to gas contamination to be negligible.

It is possible for hydrogen-scattered protons to strike the radial and conical supporting struts in the chamber and thence scatter into the counters. The corrections for these scattered protons have been estimated on the basis of Williams' equation,[22] and were less than 0.1 percent at all angles.

DETERMINATION OF GEOMETRICAL FACTORS

The basic differential equation defining scattering yields (ratio of scattered to incident protons) is

$$dY=(d\sigma/d\Omega)_{c.m.}Ndtd\Omega$$

where dY is the yield of protons scattered into the solid angle $d\Omega$ from a path length dt of incident beam. N is the number of scattering nuclei per unit volume.

Reference to Fig. 2 shows that scattering occurs over such an extended region in this apparatus that the solid angle subtended by a given counter will vary considerably over the scattering region, and hence many of the usual simplifying assumptions made in other scattering experiments are not justified here. The above quantity was integrated over the solid angle $d\Omega_{c.m.}$ and along the scattering length dt. The geometry was evaluated in terms of a factor G, defined as,

$$1/G=\int d\Omega dt.$$

Then,

$$(d\sigma/d\Omega)_{c.m.}=GY/N$$

The assumption is made that $(d\sigma/d\Omega)_{c.m.}$ is a linear function of the scattering angle θ within the range of θ accepted by a given counter, for lack of previous knowledge of the real shape of the curve. The errors introduced by this assumption are calculated to be less than $\frac{1}{2}$ percent, if one accepts the theoretical curve for $\delta_s=49°21.6'$ in Fig. 7, as the true one. Table II indicates the angular interval covered by each of the counters, ranging from 10.6° for the 27.3° counter (all angles are in center of mass system) to 19.4° for the 89.7° counter. The entire angular interval does not have the same weight of course, since relatively fewer protons of extreme angles can get in. The weighting functions for protons of various angles getting into a given counter are roughly symmetrical trapezoids as shown in Fig. 6.

For purposes of plotting the data, the effective angle of each counter is taken as half-way between the two extreme angles which the counter "sees."

The G factors were evaluated by two independent methods: first by graphical integration from an accurate full-scale drawing, and then by an analytic method. We wish to acknowledge the material assistance of Mr. F. Fillmore in developing the latter approach. The two methods agreed at all angles to better than $\frac{1}{2}$ percent. A number of small corrections to the above are necessary, due to simplifying assumptions made in the calculations. The value of these will be given for a typical counter, the 64.7° one:

1. -1.5 percent, due to scattered protons penetrating the corners of the defining cylinders (copper). It is assumed that the protons are not scattered in the copper, since roughly as many will scatter into a given counter as get scattered out. All protons are assumed to reach the counters if the thickness of copper they must penetrate leaves them enough energy to penetrate the aluminum absorber at the counter window. This energy threshold of the counters greatly reduces the effect of penetration of the copper.

2. $+0.16$ percent, caused by "tunnel effect" of the parallel sides of the apertures of the counter windows.

3. A correction for finite width of the incident beam was necessary for the small angle counters, amounting to -0.35 percent at 27.3°. The original calculations assumed the beam to be a line source.

4. It was discovered that certain dimensions of the chamber were warped when it was assembled, since it was necessary to draw the peripheral ring of bolts tight to make the major vacuum seals. Hence it was necessary to measure all the essential dimensions while it was assembled. This was done by means of various gauges inserted through the access port. The radius of the

[22] E. J. Williams, Proc. Roy. Soc. **169**, 531 (1939).

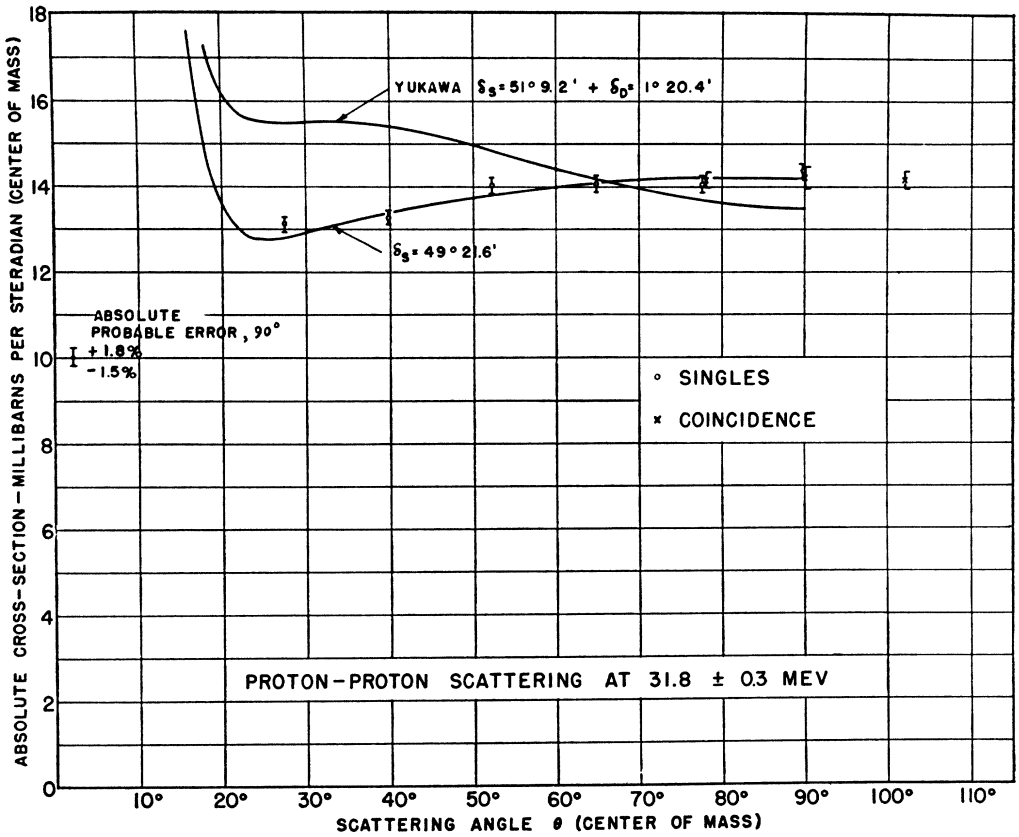

FIG. 7. Absolute differential cross-section for proton-proton scattering at 31.8±0.3 Mev. The theoretical curves are indicated by the solid lines.

counter windows from the center of the chamber was measured at six points for each counter, and the width of each counter aperture was measured at 18 points. The angular position of each counter aperture relative to the center of the chamber was measured by calipers and calculated by trigonometry. The aperture between the defining cylinders was measured, as well as their diameters and their position relative to the center of the chamber. Corrections were derived from these data for each counter, amounting to +2.4 percent for the 64.7° counter. It is believed that the result of these measurements is good to ±0.2 percent.

The corrected G factors are listed in Table I.

PROCEDURE

The alignment of collimators and the scattering chamber was accomplished as follows:

The position of the beam at the exit of the linear accelerator is determined by observing fluorescence caused by the incident protons. A limiting aperture A is then inserted, and the position of the deflected beam is observed in the region of the exit to the analyzing magnet chamber. A second limiting aperture B is inserted at this point and the position of the beam is observed in the region of the scattering chamber. Aperture C is then installed, and the axis of the deflected beam is determined by apertures B and C. Cross-hairs are installed in apertures B, C, and D, the angle-defining cylinders and the main supporting hub. Aperture D, the angle-defining cylinder, and the hub are first adjusted until coaxial. The entire scattering chamber is supported on three adjustable screws for vertical deflection. The front and back can be moved independently in a horizontal direction by means of adjusting screws and sliding planes.

With the aid of the cross-hairs and a transit-type cathetometer, the apparatus was aligned with the axis of the beam to better than ±0.010 in. The general alignment is checked by illuminating a photographic plate with the proton beam in the region of the charge integrator.

The foils were then installed in aperture D, and the chamber was filled with hydrogen (see above). The correct amplification for each counter must be determined so that all of the protons are counted but as few background counts as possible result. Since the background was due to photoelectrons and to knock-on collisions of neutrons with the walls and gas of the counters, a nearly continuous spectrum of background pulse heights was present. Increasing the gas multiplication of the counter increases the background at a very rapid rate. The technique used for setting the gas multiplication was as follows: (1) The counter apparatus was allowed to come to equilibrium by operating for an hour. (2) A pulsed signal generator was connected to the discriminator input of all 12 channels,

and the discriminators were adjusted to operate at the same predetermined pulse height. (3) The gain was measured and adjusted so that all amplifiers had nearly the same gain. (4) A high voltage from a single source was applied to the tungsten wires of each of the proportional counters. A phosphorous source of beta-rays was then placed in turn at each of the 0.001 in. dural windows in the counter (see Fig. 2). The potentiometers supplying the potentials for each wire were then adjusted to give approximately the same counting rate in each counter.

This procedure greatly facilitated the adjustment of the many counters. To make a scattering run, the above procedure was followed; the chamber was filled with hydrogen to one atmosphere; a measurement was made of the beam energy; the accelerator was adjusted to give a maximum beam through the analyzer into the charge integrator and its magnitude was then adjusted to give a satisfactory counting rate into the counters.

Before a run the shutter was opened, and the gas multiplication adjusted to the maximum value without overload. Next, the incident proton beam was intercepted by a "flip gate"; the counters were turned off; the charge collector cup was grounded; and the initial readings of the mechanical registers recorded.

To start a run, the charge collector cup was ungrounded; the counters were turned on; the "flip gate" was opened; and the run continued until a predetermined charge was collected on the cup. The time of the run, the pressure and temperature of the scattering hydrogen, and a total of 15 independent register readings were recorded (4 small angles, 3 large angle split counters, 3 coincidences, 1 accidental coincidence, and the background monitor).

The background run is then made by closing the shutter and repeating the above procedure. After the same amount of charge is collected, the counter readings were recorded. The background monitor counter readings were compared with the proton run, and a correction was made to the singles background for each counter by a factor equal to the ratio of the two background counts. Table I lists the difference between the proton run and the corrected background run, corrected to 0°C and 760 mm Hg, and for counter resolving time. (Less than 2 percent correction.) These average data weighted according to total collected charge are then multiplied by the geometrical factor G, listed below, which includes the geometrical functions required for conversion to the differential scattering cross section in the center of mass system. These conversion factors are listed in row 29 and the values of the cross sections are listed in row 30 of Table I.

To determine the plateau for counting all of the scattered protons, runs are made in turn by reducing the gas multiplication of each counter until counts are missed. The knee of the plateau is thus determined and scattering data (marked *) are then taken for values of gas multiplication well up on the plateau of the counters.

The data from which the plateau is determined, and the percent background are tabulated in Table I. The pressure of the argon-carbon dioxide counting gas mixture was reduced for row 10 and succeeding runs. Thus the plateau occurred at a lower counter potential.

RESULTS

Table I lists the number of proton counts, corrected for x-ray and neutron background, and resolving time of the counters, and normalized for a collected charge of 317×10^{-12} coulombs. The column Q gives the actual collected charge for each run and is used as the weighting factor in computing averages.

The plateau for the proportional counters was determined by the method described under *Procedure* above. Rows 1 to 8 give typical data for determining a plateau. The counter supply potential is listed for convenience. The actual wire potential was derived from a potentiometer connected to this supply and was approximately 60 percent of the recorded values.

The slope of the plateau was determined for the sum of all the counters by comparing the proton counts as a function of the counter potential. It was observed that statistically the plateau happened to decrease 1.6 percent for a 100 volt increase in wire potential. All data used in computing averages were well up on the plateau, and a reasonable probable error of +1 percent −0 percent is assumed because of uncertainty in the slope of the plateau.

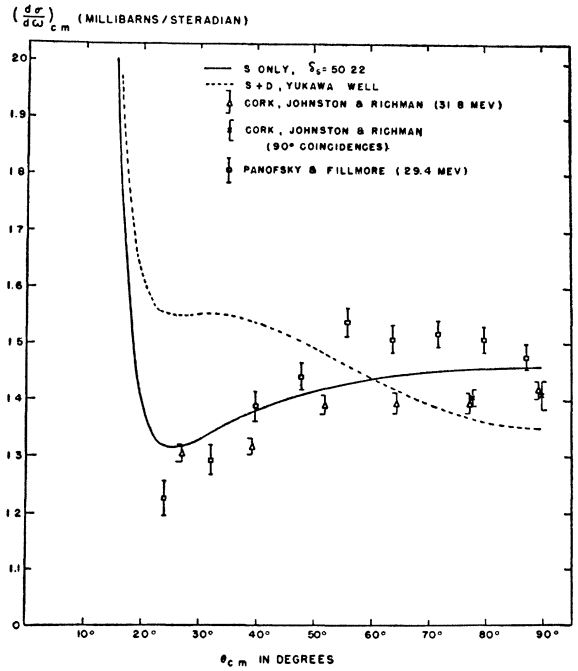

FIG. 8. Absolute differential cross-section for proton-proton scattering. The data are normalized to 32.0 Mev assuming a $1/E$ dependence of cross-section. The theoretical curves were calculated by Christian and Noyes, as follows: (a) Pure S scattering using $\delta_s=50.22°$. (b) Total singlet scattering $(S+D)$ using a Yukawa well and the same S phase shift.

The large angle counters are split into top and bottom sections. The 89.7°T and 89.7°B counters are observed to agree within statistics. After careful investigation, the particular amplifier used with the 77.6°T counter was observed to give double counts for very large input signals. The differential cross section is thus calculated using the value of counts in the 77.6°B counter.

The average background counts are listed in column 12. It is observed that the background is a rapidly changing function of the counter potential.

The mean values of proton counts weighted according to collected incident proton charge are tabulated in row 27. Row 28 is a tabulation of the percent r.m.s. deviation of the mean result. This is computed by dividing the root-mean-square deviation of the result of each series by the square root of the number of series of runs. The geometrical conversion factors are listed in row 29, and the absolute values of the differential cross section in the center of mass system are listed in row 30, expressed in millibarns (10^{-27} cm^2) per steradian. These are plotted in Fig. 7.

The assigned probable errors for 90° in the center of mass system are as follows: (a) collected charge $\pm\frac{1}{2}$ percent, (b) mean energy ± 1 percent, (c) measurement of temperature and pressure $\pm\frac{1}{3}$ percent, (d) slope of plateau (maximum) $+1$ percent, -0, (e) (percent r.m.s. deviation of counts) $\pm\frac{1}{2}$ percent, and (f) calculated geometry $\pm\frac{3}{4}$ percent.

The root sum square value of these probable errors is $+1.8$ percent, -1.5 percent, indicated by the vertical bar in Fig. 7, beside the ordinate axis.

The probable errors for the differential cross sections are the root sum square values of (d), (e), and (f) above and are indicated in Table I. Note that (e) is different at each angle.

The experiment was planned to provide two separate checks on the symmetry of scattering about 90° (center of mass), one from the single count data and one from coincidence. Singles data from the 102° counter could not be used, however, because the aluminum window could not be made quite thin enough to admit protons of maximum angle (and hence minimum energy) which the counter could "see." The coincidence geometry admits only protons of energy high enough to get into both the 78° and the 102° counters, and hence a check is provided. The close agreement between the 77.6° singles data and the 78°–102° coincidence data indicates that the measured cross section at 102° is probably not smaller than that at 78° by more than 1 percent. The coincidence data are also given in Table I.

The results indicated by Fig. 7 are different from the results expected, if one assumes the usual static potential theory. The theoretical curve for an S-wave phase shift of $\delta_s = 49°21.6'$ is included. Also, the theoretical curve, if one assumes a Yukawa potential well adjusted to fit the low energy data and having $\delta_s = 51°9.2'$ plus a $\delta_D = 1°20.4'$, is plotted in Fig. 7. A comparison with the data using the photographic emulsion detectors is given by Fig. 8.

The analysis of these data, given in a paper by Christian and Noyes in this issue of *The Physical Review* shows that the shape of the differential cross section curve is compatible with pure S-wave scattering.

Christian and Noyes show that, if one compares the proton-proton scattering at 32 Mev with the neutron-proton scattering data obtained with 40 Mev incident neutrons, one must conclude that the hypothesis of the charge independence of nuclear forces is not valid. Furthermore the absence of a repulsive force in the P state coupled with the fact that in the case of the $n-p$ interaction the repulsive forces are weak makes it difficult to understand the saturation of nuclear forces.

ACKNOWLEDGMENTS

We are greatly indebted to Mr. Edward Day for the mechanical design of the scattering chamber, to Mr. John Harvie's shop for the accurate construction of the mechanical apparatus, and to the linear accelerator crew for careful operation of the machine.The authors have profited from many stimulating discussions with Professor Robert Serber, Dr. Geoffery Chew, Mr. Richard Christian, and Mr. Pierre Noyes. It is a pleasure to thank Professor L. W. Alvarez for much helpful guidance and for suggesting the problem. We wish to thank Professor E. O. Lawrence for continued encouragement and interest in the work.